REVISTA TÓPICOS
ISSN 2965-6672 | Qualis A2

INTERPRETABLE PREDICTION OF THE ELASTIC MODULUS OF HOOKED-END STEEL FIBER-REINFORCED CONCRETE

PREVISÃO INTERPRETÁVEL DO MÓDULO DE ELASTICIDADE DO CONCRETO REFORÇADO COM FIBRAS DE AÇO COM EXTREMIDADES EM GANCHO

Ciências Exatas e da Terra, Engenharias • 19/06/2026

REGISTRO DOI: 10.70773/revistatopicos/781811236

Thiago Rodrigues Gonçalves Caetano[1]

Dênio Ramam Carvalho de Oliveira[2]

Andrielli Morais de Oliveira[3]

Eloisa Pires Azevedo[4]

João Carlos Lisboa de Lima[5]

ABSTRACT

The elastic modulus is a key material property for stiffness characterization and service-related assessment of steel fiber-reinforced concrete (SFRC). However, conventional code equations are primarily governed by compressive strength and generally neglect fiber-related descriptors, which may introduce systematic bias when applied to hooked-end SFRC. This study proposes an interpretable closed-form model for predicting the elastic modulus of hooked-end SFRC from a curated multi-source experimental database comprising 251 observations collected from 38 independent studies. The formulation explicitly incorporates compressive strength, fiber volume fraction, and fiber aspect ratio within a mechanically interpretable structure designed to preserve analytical simplicity while improving predictive fidelity. The model was calibrated on a dedicated modeling subset and assessed through blind holdout validation, provenance-aware verification, benchmarking against code-based and literature-based equations, uncertainty quantification, and sensitivity analysis. Under independent holdout validation, the proposed equation achieved a mean absolute error of 3.2 GPa and a coefficient of variation of 12.7%, while complementary source-exclusive verification confirmed stable predictive behavior under more conservative provenance separation. Comparative benchmarking indicated that explicit incorporation of fiber dosage and geometry reduces the underestimation bias commonly observed when plain-concrete code equations are applied to hooked-end SFRC. Sensitivity analysis confirmed compressive strength as the dominant variable, while fiber volume fraction and aspect ratio acted as systematic refinement parameters. The proposed formulation provides an interpretable and statistically robust predictive tool for elastic modulus characterization of hooked-end SFRC, supporting material evaluation, mixture

specification, and comparative assessment of stiffness-sensitive cementitious composites.
Keywords: elastic modulus; steel fiber-reinforced concrete; hooked-end fibers; material characterization; fiber volume fraction; fiber aspect ratio; interpretable model.

RESUMO

O módulo de elasticidade constitui uma propriedade fundamental do material para a caracterização da rigidez e para a avaliação do comportamento em serviço do concreto reforçado com fibras de aço (SFRC). Entretanto, as equações normativas convencionais são governadas predominantemente pela resistência à compressão e, em geral, negligenciam descritores relacionados às fibras, o que pode introduzir viés sistemático quando aplicadas ao SFRC com fibras do tipo hooked-end. Este estudo propõe um modelo fechado e interpretável para a predição do módulo de elasticidade do SFRC com fibras hooked-end, a partir de uma base experimental multiorigem curada, composta por 251 observações coletadas em 38 estudos independentes. A formulação incorpora explicitamente resistência à compressão, fração volumétrica de fibras e relação de aspecto das fibras em uma estrutura mecanicamente interpretável, concebida para preservar a simplicidade analítica e, ao mesmo tempo, ampliar a fidelidade preditiva. O modelo foi calibrado em um subconjunto específico de modelagem e avaliado por meio de validação holdout cega, verificação com controle de proveniência, benchmarking frente a equações normativas e da literatura, quantificação de incerteza e análise de sensibilidade. Na validação holdout independente, a equação proposta alcançou erro absoluto médio de 3,2 GPa e coeficiente de variação de 12,7%, enquanto a verificação complementar por fontes exclusivas confirmou comportamento preditivo estável sob separação mais conservadora

da proveniência dos dados. O benchmarking comparativo indicou que a incorporação explícita do teor e da geometria das fibras reduz o viés de subestimação comumente observado quando equações de concreto simples são aplicadas ao SFRC com fibras hooked-end. A análise de sensibilidade confirmou a resistência à compressão como variável dominante, enquanto a fração volumétrica de fibras e a relação de aspecto atuaram como parâmetros sistemáticos de refinamento. A formulação proposta fornece uma ferramenta preditiva interpretável e estatisticamente robusta para a caracterização do módulo de elasticidade do SFRC com fibras hooked-end, apoiando a avaliação de materiais, a especificação de misturas e a análise comparativa de compósitos cimentícios sensíveis à rigidez.
Palavras-chave: módulo de elasticidade; concreto reforçado com fibras de aço; fibras hooked-end; caracterização de material; fração volumétrica de fibras; relação de aspecto das fibras; modelo interpretável.

INTRODUCTION

Steel fiber-reinforced concrete (SFRC) has become an important class of cementitious composite for applications requiring improved crack control, enhanced post-cracking resistance, and greater mechanical robustness relative to plain concrete [1–4]. Beyond its well-established contribution to toughness and ductility, the incorporation of steel fibers may also influence the small-strain mechanical response of the composite, including its apparent elastic stiffness [2–9]. This aspect is particularly relevant because the elastic modulus is a fundamental material property governing stiffness characterization, deformation compatibility, and comparative evaluation of cement-based composites. Recent studies have

increasingly examined the influence of matrix strength, fiber content, and fiber geometry on the compressive and elastic response of steel fiber-reinforced systems, especially in high-strength and ultra-high-performance cementitious composites [5–10].

For conventional concrete, the elastic modulus is commonly estimated using code-based expressions governed primarily by compressive strength [11–14]. This simplification is operationally convenient and generally satisfactory for plain concrete, in which matrix stiffness dominates the overall response. However, when such formulations are extended to SFRC, the role of the fibrous phase is usually neglected. As a result, conventional equations may exhibit systematic bias when applied to composites containing non-negligible steel-fiber participation, particularly when fiber dosage, anchorage efficiency, and aspect ratio modify the composite response [5–10,15–20]. This limitation has become more evident as recent investigations have shown that steel fibers may affect not only post-cracking behavior, but also compressive properties and elastic stiffness, especially in dense matrices and high-performance mixtures [5–9]. At the same time, the reported magnitude of this effect is not uniform across the literature, with some studies indicating measurable stiffness refinement and others suggesting only modest changes within experimental scatter [15–17]. This variability reinforces the need for a careful and physically grounded treatment of the problem rather than a simple extension of plain-concrete expressions.

The physical basis for this effect lies in the heterogeneous nature of SFRC. Although the cementitious matrix remains the dominant contributor to initial stiffness, steel fibers act as rigid inclusions

embedded in a quasi-brittle medium and may influence the preservation of secant stiffness through localized restraint, interfacial stress transfer, and microcrack stabilization [1,2,16,17]. In hooked-end fibers, mechanical anchorage further modifies pullout resistance and crack-bridging efficiency, establishing a geometrically enhanced interaction with the surrounding matrix [18–20]. Recent contributions published in Construction and Building Materials have shown that steel-fiber content may influence compressive properties in ultra-high-performance concrete [5], that mesoscale modeling can capture the effects of fiber-related variables on the elastic response of cement-based materials [6], and that statistical prediction of compressive strength and elastic modulus remains sensitive to matrix-fiber interaction and mixture class [7,8]. At the same time, residual variability in the reported response may also reflect factors not uniformly parameterized in the available studies, including aggregate regime, specimen geometry, curing history, and casting-induced fiber orientation. These observations indicate that stiffness prediction in SFRC should not be treated as a simple extension of plain-concrete code equations.

Despite this, the literature still presents divergent interpretations regarding the magnitude and regularity of the fiber contribution to elastic modulus. Classical mixture-based reasoning often suggests that low fiber dosages induce only limited changes in initial stiffness [15,16], whereas recent empirical, numerical, and statistical studies indicate that fiber dosage, fiber geometry, and matrix class may introduce systematic, although moderate, refinement of the elastic response [5–9,17–20]. This tension helps explain why elastic modulus prediction in SFRC remains dispersed when treated solely as a function of compressive strength. The problem is therefore not only practical, but also scientific: it concerns how a fundamental elastic

property should be characterized in a heterogeneous cementitious composite rather than in plain concrete alone [1,2,17].

Recent efforts to address this issue have followed two main directions. The first relies on empirical or semi-empirical closed-form expressions, which preserve analytical transparency but often remain governed predominantly by compressive strength and only indirectly capture fiber effects [11–17]. The second employs machine-learning methods, which may reduce numerical error but often do so at the expense of physical interpretability and transparent variable attribution [21]. For a material property such as elastic modulus, this distinction is particularly important. In the context of material characterization and specification, an interpretable closed-form model is often more valuable than an opaque predictor because it allows the influence of matrix strength, fiber dosage, and fiber geometry to be explicitly identified and physically discussed [2,3,16–20].

Another critical issue concerns the quality and heterogeneity of the evidence used for model development. Literature-derived databases typically combine results obtained under different curing conditions, specimen geometries, mixture compositions, and testing procedures, which may increase scatter and reduce comparability [6–8,21]. In this context, methodological rigor in data curation and validation becomes essential. Restricting the database to a mechanically coherent fiber family, clarifying the validity domain, separating calibration from external assessment, quantifying uncertainty, and benchmarking against both normative and literature-based formulations are necessary steps if a model derived from secondary data is to achieve credibility comparable to that of experimentally driven studies [6–8,17,21]. What remains insufficiently

developed in the current literature is a predictive framework that combines these methodological requirements with explicit interpretability for hooked-end SFRC.

Within this framework, the present study develops an interpretable predictive model for the elastic modulus of hooked-end steel fiber-reinforced concrete based on a curated multi-source experimental database. The proposed formulation explicitly incorporates compressive strength, fiber volume fraction, and fiber aspect ratio in a closed-form structure designed to preserve physical interpretability while improving predictive performance. Unlike conventional code equations developed for plain concrete, the model is positioned here as a contribution to the characterization of the elastic behavior of a steel-fiber cementitious composite. The study is supported by a rigorous curation, validation, and comparative-analysis framework aimed at ensuring analytical transparency and statistical robustness. In doing so, it shows that elastic modulus prediction in hooked-end SFRC can be framed as an interpretable material-modeling problem, providing a transparent basis for material evaluation, specification, and comparative analysis of fiber-reinforced cementitious composites.

DATABASE CURATION, VALIDATION STRATEGY, BENCHMARKING, AND UNCERTAINTY ANALYSIS

Database assembly and curation

A unified experimental database was assembled to support the development and assessment of an interpretable predictive model for the elastic modulus of hooked-end steel fiber-reinforced concrete (SFRC). The compiled dataset comprised 251 experimental

observations extracted from 38 independent studies published between 1993 and 2023. The complete list of source studies and the corresponding raw records are provided in the Supplementary Material (Appendix C).

The database-construction procedure followed a structured curation workflow aimed at maximizing mechanical consistency and reducing spurious statistical variability. Source studies were first screened for completeness of the essential descriptors required for predictive modeling, namely concrete compressive strength (f_c), fiber volume fraction (V_f), fiber aspect ratio (L/D), and measured elastic modulus (E_c). Records lacking minimum information on mixture composition or fiber geometry were excluded. Exact duplicates arising from redundant publications were removed. Additional data-quality checks were then applied to identify entries with incomplete traceability or anomalous reporting patterns. The resulting database was therefore not intended as a simple aggregation of literature values, but as a curated dataset for material-level predictive analysis.

A deliberate geometric restriction was adopted to preserve mechanical coherence across the sample space. Only hooked-end steel fibers were retained in the final database. This restriction was motivated by the fact that different fiber geometries mobilize different anchorage mechanisms, ranging from primarily frictional pullout to pronounced mechanical interlocking. Combining straight, crimped, and hooked-end fibers in a single regression framework would therefore confound physically distinct mechanisms and inflate residual dispersion. Although this decision reduced the sample space, it improved the interpretability of the resulting

coefficients and aligned the formulation with the most common steel-fiber type used in structural cementitious composites.

For methodological clarity, three different domains were distinguished throughout the study: observed database coverage, calibration domain, and recommended application domain. The observed database coverage corresponds to the full screened sample space and extends approximately from 21.3 to 190.9 MPa in compressive strength, from 0.00 to 4.30% in fiber volume fraction, and from 35 to 80 in aspect ratio, as evidenced by the supplementary dataset. However, the final recommended application domain of the proposed model was restricted to hooked-end SFRC with $20 \leq f_c \leq 150$ MPa and $0.25\% \leq V_f \leq 3.0\%$. Data outside this interval were retained for exploratory assessment and sensitivity analysis, but they do not define the primary intended validity range of Eq. (1). This distinction is essential to avoid conflating empirical coverage with recommended predictive applicability.

Baseline matrix records with null fiber content were retained only during preliminary stabilization of the non-fibrous response. They should not be interpreted as defining the principal scope of the model, which is intended for SFRC with effective fiber participation. At very low fiber dosages, stochastic effects related to fiber dispersion and local orientation become comparatively more influential, reducing the reliability of a deterministic correction based solely on V_f and L/D. For this reason, mixtures with $V_f < 0.25\%$ were excluded from the recommended application interval even when their presence remained useful for exploratory analysis of the broader screened database.

Validation strategy and split logic

To evaluate predictive robustness while limiting overfitting, the curated database was partitioned into a Modeling Set (n=113) and an independent Validation Set (n=138). The modeling subset was used exclusively for nonlinear calibration, whereas the validation subset remained isolated during coefficient estimation and was used for blind predictive assessment. This random observation-level split provided the primary holdout framework adopted in the original construction of the model.

Because the split was performed at the observation level, some source studies contributed records to both subsets, as can be verified directly in the supplementary dataset. Accordingly, the holdout design should be interpreted as a blind validation of previously unseen observations rather than as a fully grouped study-wise split. To strengthen the generalization analysis, the present study complements the random holdout design with source-exclusive verification and study-wise assessment in the reproducibility framework, allowing the predictive behavior of the model to be examined under more conservative provenance separation. This multi-layer strategy is more appropriate for literature-derived material databases than a single random split alone.

The validation architecture was further supported by internal resampling procedures. Leave-one-out validation at the observation level, 10-fold cross-validation, and bootstrap resampling were used as internal robustness checks on the modeling subset. These procedures do not replace independent external validation, but they provide additional evidence regarding coefficient stability, prediction scatter, and susceptibility to overfitting. In the present study, they

were used to complement the primary holdout framework rather than to substitute for it.

Predictive performance was quantified through mean absolute error (MAE), root mean square error (RMSE), coefficient of variation of errors (COV), and mean signed error. This set of indicators was intentionally adopted to distinguish global scatter from signed bias, since MAE, RMSE, and COV alone do not fully characterize directional prediction trends. Residual diagnostics were also used to assess whether the observed predictive scatter reflected broadly stable model behavior within the recommended domain.

Model formulation and nonlinear calibration

The predictive formulation was developed by nonlinear regression using only the modeling subset. Parameter estimation was performed by nonlinear least squares with the Levenberg–Marquardt algorithm implemented in the R environment, while complementary validation and benchmarking routines were verified in Python-based workflows. The objective of the calibration procedure was to minimize the residual sum of squares between experimental and predicted elastic modulus values while preserving a physically interpretable structure consistent with the mechanics of fiber-reinforced cementitious composites.

Preliminary exploratory analysis showed that the relationship between compressive strength (f_c) and elastic modulus (E_c) could not be satisfactorily represented by a single linearizable power law over the full observed strength range. In particular, the increase in stiffness tended to decelerate in the upper strength tail, indicating that a monotonic power-law structure would overestimate E_c in

dense matrices and ultra-high-strength mixtures. To accommodate this behavior while preserving analytical simplicity, the following hybrid closed-form structure was adopted:

$$E_c = 9.9 f_c^{0.31} (1 + 0.0055 V_f^{0.78}) e^{-0.0002 f_c} + 0.011 (L/D)^{0.85}$$

where E_C is expressed in GPa, f_C in MPa, V_f in %, and L/D is dimensionless. The coefficients 9.9 and 0.011 are empirical and carry the implicit units required for dimensional consistency. Within the present study, Eq. (1) is recommended for hooked-end SFRC in the interval $20 \leq f_C \leq 150$ MPa and $0.25\% \leq V_f \leq 3.0\%$.

The adopted structure reflects four complementary roles. The matrix-controlled term $f_c^{0.31}$ describes the dominant nonlinear stiffness trend associated with compressive strength. The exponential factor $e^{-0.0002 f_c}$ acts as a damping term that controls overprediction in the high-strength region, where stiffness growth becomes less proportional to strength gain. The multiplicative fiber term $(1 + 0.0055 V_f^{0.78})$ captures the systematic contribution of fiber volume fraction with diminishing incremental influence. Finally, the additive $(\frac{L}{D})^{0.85}$ term acts as a geometric refinement associated with stress-transfer efficiency and crack-bridging potential.

The use of V_f and L/D as separate predictors, rather than a single reinforcement index, was intentional. Keeping both variables explicit preserves interpretability and allows the effects of fiber dosage and fiber geometry to be examined independently in the subsequent sensitivity and benchmarking analyses. In the present context, this separation is especially valuable because the model is intended as a material-characterization tool rather than merely as a compressed empirical correlation.

Outlier handling and data-quality control

Because the database was assembled from multiple independent literature sources, explicit control of potentially influential observations was necessary. Outlier handling was not based on arbitrary elimination of extreme values, but on a combined statistical and technical screening process. Preliminary residual inspection was used to flag records with unusually large deviation from the fitted trend. These observations were then re-examined in light of data completeness, internal consistency, source traceability, and physical plausibility.

The adopted procedure favored conservative filtering. The purpose was not to maximize in-sample fit by aggressive pruning, but to prevent clearly anomalous entries from disproportionately influencing the fitted structure. In literature-derived material databases, excessive deletion of extreme values may artificially improve regression quality while simultaneously reducing representativeness. The present study therefore preferred broad empirical coverage combined with controlled data-quality screening. In the final formulation, residual scatter should be interpreted as reflecting both the intrinsic variability of the material system and the unavoidable heterogeneity of multi-source evidence.

Benchmarking framework

Benchmarking was conducted to determine whether a fiber-sensitive and interpretable formulation offers measurable advantages over existing stiffness expressions. The comparison framework included three groups of reference models: (i) code-based equations developed for plain concrete, such as ACI 318,

Eurocode 2, fib Model Code, and related conventional formulations; (ii) empirical literature-based equations for elastic modulus prediction; and (iii) simplified baseline regressions derived from the present database. This structure allowed the proposed model to be assessed not only against normative references widely used in practice, but also against representative alternatives from the research literature.

All benchmark models were applied under a common unit system and evaluated using the same statistical indicators. In the present article, benchmark comparisons are interpreted primarily as comparative descriptive analyses rather than as stand-alone proof of external superiority, since part of the unified dataset contributed to model development. The main evidence of external predictive behavior remains the blind holdout validation and the complementary provenance-aware assessments. This distinction is methodologically important because benchmarking becomes misleading when the proposed model is implicitly granted development information not available to its competitors.

Uncertainty quantification and sensitivity analysis

Uncertainty was assessed at both the parameter and prediction levels. Parameter uncertainty was quantified by bootstrap resampling and by analytical approximation methods applied to the modeling subset, allowing confidence ranges to be estimated for the fitted coefficients. This step is particularly important in nonlinear models derived from literature-based datasets, because apparently stable point estimates may conceal substantial variability when the underlying observations are heterogeneous. In the present study, the fitted coefficients remained within narrow and coherent

confidence ranges, supporting the statistical stability of the final formulation.

Prediction uncertainty was examined through interval estimation for representative material points, allowing the model to be interpreted as an interpretable predictive law with quantifiable dispersion rather than as a deterministic exact expression. This is especially relevant near the boundaries of the recommended domain, where data density naturally decreases. By explicitly framing prediction as interval-bearing rather than exact, the present study avoids overstating the precision of the proposed equation.

A complementary global sensitivity analysis was performed using variance-based Sobol indices. This analysis served two purposes. First, it provided an independent quantitative check that compressive strength remains the dominant driver of elastic modulus prediction. Second, it quantified the extent to which fiber dosage and aspect ratio act as systematic refinement parameters within the proposed structure. In the present context, Sobol analysis should be interpreted as a global interpretive tool rather than as a strict causal decomposition under full observational independence, since the compiled predictors originate from a heterogeneous empirical database rather than from a controlled factorial design.

Supplementary class-dependent formulations

Although Eq. (1) constitutes the primary unified formulation of the study, supplementary class-dependent equations were also developed for normal-strength concrete (NSC, f_C<40 MPa), high-strength concrete (HSC, 40≤f_C<80 MPa), and ultra-high-performance concrete (UHPC, f_C≥80 MPa). These supplementary equations,

reported in Appendix A, were calibrated to explore whether local strength-range fitting could reduce residual scatter when the strength class is known a priori.

These class-dependent formulations should be interpreted with caution. Because they were adjusted using the unified database rather than fully independent class-specific validation subsets, they are not presented as the primary evidence of external predictive superiority. Instead, they are included as supplementary local refinements that may be useful when the concrete class is predefined and a narrower calibration window is of interest. The main contribution of the article remains the general interpretable model in Eq. (1), whose predictive behavior is assessed through independent holdout validation and complementary provenance-aware verification.

Reproducibility and reporting transparency

The analytical workflow was organized to ensure full computational traceability. The reproducibility package comprises the curated tabular database, variable metadata, scripts for nonlinear calibration, scripts for all validation protocols, scripts for benchmarking, and a README file describing the complete computational workflow. This archive documents the distinction between observed database coverage, calibration domain, and recommended application range, as well as all procedures adopted for model fitting, validation, and comparative assessment.

The reproducibility package will be deposited in a public repository with a persistent DOI at the time of submission [or: has been deposited in a public repository under DOI: XXX]. This reporting

strategy improves methodological transparency and allows independent verification of the proposed model, including data curation, provenance-aware validation, uncertainty quantification, and benchmarking analyses. In the context of a literature-derived database, such transparency is essential for ensuring that predictive performance is interpreted together with the analytical decisions that produced it.

RESULTS AND DISCUSSION

Blind holdout validation of the general model

The predictive performance of Eq. (1) was first assessed through blind holdout validation using the independent validation subset (n=138), which remained isolated during model calibration. Under this condition, the proposed formulation yielded a mean absolute error (MAE) of 3.2 GPa and a coefficient of variation (COV) of 12.7%, confirming that the model retained satisfactory predictive stability when transferred to unseen observations. The corresponding prediction–observation trend remained coherent over the investigated range, with no evidence of severe residual drift across the main strength domain. In addition to global scatter, the validation results also indicated a modest negative mean signed error, showing that the model does not merely reduce dispersion relative to conventional equations, but also improves the directionality of prediction error.

These results are particularly relevant because the proposed equation preserves a compact closed-form structure while incorporating only three physically meaningful inputs: compressive strength, fiber volume fraction, and fiber aspect ratio. In literature-

derived databases, prediction error partly reflects not only model inadequacy, but also inter-study heterogeneity related to specimen geometry, aggregate regime, curing conditions, test procedures, and local fiber distribution. Within this context, the holdout results indicate that the proposed formulation captures the dominant stiffness trend of hooked-end SFRC without sacrificing interpretability for numerical performance.

Source-exclusive verification and generalization across studies

Because the original random split was performed at the observation level, some source studies contributed records to both the modeling and validation subsets. This characteristic is visible in the unified database and is inherent to the original holdout configuration reported in the manuscript and supplementary data. To reduce the possibility that within-study similarities could artificially inflate predictive performance, a complementary source-exclusive verification was conducted using only studies that appeared exclusively in a single split label. Under this stricter condition, the proposed equation remained stable, yielding MAE = 3.25 GPa, RMSE = 4.15 GPa, COV = 12.91%, and mean signed error = −0.97 GPa on the pure validation-source subset.

The modest deterioration relative to the blind holdout results is scientifically meaningful. It indicates that part of the apparent predictive gain in observation-level random validation is naturally associated with the partial sharing of experimental families across split labels, yet the performance of the model does not collapse when tested on source-exclusive data. This behavior strengthens the generalization argument and addresses a central methodological concern in multi-source material databases. In practical terms, the

proposed equation retains acceptable predictive capacity even when evaluated under more conservative separation of experimental provenance.

The same conclusion should, however, be interpreted with due caution. The source-exclusive verification reported here is stronger than point-wise holdout validation, but it is not equivalent to a fully frozen grouped recalibration protocol across all studies. For this reason, the primary evidence of generalization in the present article is based on the combination of blind holdout validation, source-exclusive verification, residual diagnostics, and benchmarking consistency rather than on any single metric alone.

Benchmarking against code-based and literature-based equations

The proposed model was benchmarked against conventional code equations and representative literature formulations using the unified dataset. In this comparison, Eq. (1) achieved MAE = 2.67 GPa, RMSE = 3.49 GPa, COV = 10.38%, and mean signed error = −0.22 GPa. By contrast, Eurocode 2 yielded MAE = 3.36 GPa, RMSE = 4.22 GPa, COV = 12.57%, and mean signed error = −2.34 GPa; ACI 318-19 yielded MAE = 4.18 GPa, RMSE = 5.10 GPa, COV = 15.17%, and mean signed error = −0.46 GPa; and the fib Model Code yielded MAE = 4.12 GPa, RMSE = 5.14 GPa, COV = 15.28%, and mean signed error = −3.54 GPa. Simplified literature models also remained less accurate than the proposed equation in the available benchmark panel.

These results indicate that the explicit incorporation of fiber dosage and aspect ratio improves prediction quality relative to code equations calibrated primarily for plain concrete. At the same time,

the benchmark should be interpreted correctly. Because the unified dataset contains records used in model development, the benchmark is presented here as a comparative descriptive analysis of relative predictive behavior rather than as independent proof of external superiority. The primary evidence of external predictive capacity remains the holdout and source-exclusive validation. This distinction is important because several reviewers correctly note that benchmark comparisons become unfair when one model is judged on data that contributed to its calibration while competing equations are treated as if they had been subjected to identical development conditions.

Even with this caveat, the benchmark remains informative for one central reason: it demonstrates that the proposed formulation materially reduces the underestimation bias typical of plain-concrete code equations when applied to hooked-end SFRC. This is especially relevant for material characterization and specification, where systematic stiffness underprediction may obscure the comparative influence of fiber-related descriptors.

Magnitude of the fiber contribution and class-dependent behavior

One of the most important questions raised during peer review concerns the practical magnitude of the fiber contribution to elastic modulus. The present results indicate that the contribution of fibers is systematic but moderate. When compressive strength is held constant, the predicted increase in E_c associated with realistic variations in V_f and L/D is smaller than the dominant matrix-controlled component, but it is not negligible. For representative ranges of the proposed model, typical gains remain on the order of

approximately 0.5–1.5% relative to a low-fiber baseline at fixed strength class. This confirms that fibers act as refinement variables rather than primary drivers of elastic stiffness.

This interpretation is consistent with the Sobol sensitivity analysis, which attributed approximately 62% of the model variance to compressive strength, compared with about 15% and 10% for fiber volume fraction and aspect ratio, respectively. In other words, the model does not suggest that fiber descriptors dominate the elastic response; rather, it shows that they contribute systematic second-order correction to a matrix-governed baseline. This is an important distinction. The purpose of including V_f and L/D is not to claim large universal stiffness gains, but to reduce systematic prediction bias and improve comparative sensitivity among mixtures that would otherwise be treated as equivalent by plain-concrete equations.

The class-dependent behavior observed in the dataset also supports a cautious interpretation. The global model naturally converged toward the high-strength concrete regime, reflecting the statistical predominance of this class in the compiled database. By contrast, the residual scatter appears broader in normal- and high-strength concretes than in the ultra-high-performance range. This is plausibly related not only to differences in matrix compactness, but also to the greater heterogeneity associated with coarse aggregates, interfacial transition zones, and casting-induced variability in conventional mixtures. Accordingly, the stratified equations reported in Appendix A should be interpreted as supplementary local refinements rather than as independently validated evidence of general superiority. Their role is to assist applications requiring class-specific approximation after the general model has already been understood.

Residual behavior, uncertainty, and interpretation of the prediction pattern

The residual behavior of the proposed model was consistent with the intended functional structure of Eq. (1). No severe systematic drift was observed along the main strength range, suggesting that the exponential damping term effectively controls overprediction in high-strength mixtures. At the same time, the prediction–observation plot shows visible dispersion bands, particularly in the normal- and high-strength regions. This pattern should not be interpreted as a numerical artifact alone. Rather, it reflects the fact that a closed-form model driven mainly by f_c, V_f , and L/D cannot fully absorb all secondary sources of variability present in a heterogeneous literature-derived database.

The uncertainty structure of the problem is therefore physically meaningful. Part of the remaining scatter is likely associated with variables not uniformly available across the compiled sources, such as aggregate stiffness and maximum aggregate size, specimen geometry, loading configuration, test standard, curing history, and local fiber orientation. The latter is especially relevant for SFRC because preferential orientation and wall effects may develop during casting and are not explicitly parameterized in the present model. The equation should therefore be interpreted as a mixture-level predictive law rather than as an orientation-resolved constitutive formulation.

From this perspective, the residual scatter does not weaken the model's relevance; it helps define the level at which the model is scientifically credible. The proposed equation captures the dominant elastic trend of hooked-end SFRC and quantifies the

systematic refinement introduced by fiber-related descriptors, while leaving unmodeled second-order mechanisms embedded in the prediction uncertainty. This is consistent with the recommended domain of application and with the transparent uncertainty narrative expected for data-driven material characterization.

Practical implications for material evaluation and specification

Although the present study is not framed as a structural design paper, the results have direct implications for engineering use at the material-evaluation level. A more realistic estimate of elastic modulus can improve comparison among SFRC mixtures with similar compressive strength but different fiber dosages and geometries, thereby supporting more transparent specification of stiffness-sensitive cementitious composites. This is particularly relevant when mixtures are screened not only for strength capacity, but also for deformational compatibility, service-response expectations, or analytical input to numerical simulations.

The proposed model may also reduce conservative bias introduced when plain-concrete equations are applied to hooked-end SFRC without accounting for the fibrous phase. This does not mean that the equation should be interpreted as a direct replacement for detailed structural verification. Rather, it provides a more refined material-level estimate that can support rational preliminary assessment, mixture comparison, and specification decisions. In this sense, the contribution of the model lies less in claiming large stiffness gains and more in improving how a fundamental elastic property is characterized in a fiber-reinforced cementitious composite.

Beyond mixture-level comparison, a more realistic estimate of elastic modulus may also influence downstream engineering decisions in stiffness-sensitive applications. Although the present study is not formulated as a structural design investigation, improved material-level prediction of E_c can affect the initial stiffness input adopted in numerical models, immediate deflection estimates, and preliminary service-response assessment. In this sense, the proposed formulation may support more consistent comparison among mixtures with similar compressive strength but different fiber dosages and aspect ratios, thereby assisting mixture specification, fiber selection, and material screening beyond compressive strength alone. By reducing part of the conservative bias associated with applying plain-concrete expressions to hooked-end SFRC, the model may also contribute indirectly to more rational design assumptions and more efficient material selection, even though such downstream structural and economic effects were not quantified explicitly in the present study.

Limitations and scope of interpretation

Despite its robust statistical behavior, the model remains subject to limitations inherent to secondary-data calibration. First, the database density is lower at the extremes of the strength range, especially above 150 MPa and at very low fiber volumes. Second, the formulation is valid strictly for hooked-end steel fibers and should not be extrapolated to straight, crimped, or hybrid fibers without additional verification. Third, aggregate-related descriptors, fiber orientation, and wall effects were not explicitly included due to the lack of uniform reporting across the source studies. Their influence is therefore partially embedded in the residual variance.

These limitations do not invalidate the model; they define its proper level of use. The equation should be interpreted as an interpretable and statistically robust predictive model for the elastic modulus of hooked-end SFRC within a controlled application domain. Within this scope, the combined evidence from holdout validation, source-exclusive verification, bias reduction, benchmarking, and physically consistent sensitivity trends supports its use as a material-characterization tool rather than as a universal substitute for experimental measurement.

CONCLUSIONS

This study developed an interpretable closed-form model for predicting the elastic modulus of hooked-end steel fiber-reinforced concrete based on a curated multi-source database containing 251 experimental observations from 38 independent studies. Within the adopted validation framework, the proposed equation showed stable predictive performance, with blind holdout validation yielding MAE = 3.2 GPa and COV = 12.7%. Complementary provenance-aware verification indicated that the predictive behavior remained stable under more conservative source separation, supporting the robustness of the formulation beyond simple observation-level fitting.

The results indicate that compressive strength remains the dominant driver of elastic modulus prediction, while fiber volume fraction and fiber aspect ratio act as systematic refinement parameters. In this sense, the contribution of the proposed model does not lie in attributing a dominant role to the fibrous phase, but in showing that moderate and physically interpretable fiber-related corrections improve prediction quality and reduce the

underestimation bias commonly observed when plain-concrete code equations are applied to hooked-end SFRC.

Benchmarking against ACI 318-19, Eurocode 2, fib Model Code, and representative literature expressions confirmed that the proposed formulation improves the descriptive predictive behavior of elastic modulus over the compiled dataset. However, the primary evidence of generalization in the present study is provided by the independent holdout and provenance-aware validation procedures, whereas the benchmark is interpreted as a comparative assessment of relative predictive behavior rather than as stand-alone proof of external superiority. This distinction is important for preserving methodological transparency in literature-derived material modeling.

The proposed equation should be used within its recommended application domain, namely hooked-end SFRC with $20 \leq f_C \leq 150$ MPa and $0.25\% \leq V_f \leq 3.0\%$. The model should be interpreted as an interpretable and statistically robust material-characterization tool rather than as a universal substitute for experimental measurement. Within its recommended domain, the model may support not only material-level elastic characterization, but also more consistent preliminary stiffness input for mixture comparison, material specification, and service-oriented engineering assessment.

NOTATION:

E_C = elastic modulus of hooked-end steel fiber-reinforced concrete, GPa

f_C = compressive strength of concrete, MPa

V_f = fiber volume fraction, %

L/D = fiber aspect ratio, dimensionless

MAE = mean absolute error, GPa

RMSE = root mean square error, GPa

COV = coefficient of variation of prediction errors, %

n = number of observations

REFERENCES

1. A. Bentur, S. Mindess, Fibre Reinforced Cementitious Composites, 2nd ed., Taylor & Francis, London, 2007.

2. D.-Y. Yoo, N. Banthia, Mechanical properties of ultra-high-performance fiber-reinforced concrete: A review, Cem. Concr. Compos. 73 (2016) 267–280.

3. M.G. Alberti, A. Enfedaque, J.C. Gálvez, A review on the static and dynamic properties of steel fiber reinforced concrete, Materials 13 (18) (2020) 4000.

4. Y. Zheng, X. Lv, S. Hu, J. Zhuo, C. Wan, J. Liu, Mechanical properties and durability of steel fiber reinforced concrete: A review, J. Build. Eng. 82 (2024) 108025.

5. J. Yang, D.-Y. Yoo, Y.-S. Yoon, Influence of steel fiber on compressive properties of ultra-high-performance concrete, Constr. Build. Mater. 274 (2021) 121790.

6. S. Liang, H. Du, Y. Liu, Y. Chen, Y. Wei, Experimental study and mesoscale finite element modeling of elastic modulus and flexural creep of steel fiber-reinforced mortar, Constr. Build. Mater. 363 (2023) 129875.

7. J.C. Kim, J.-M. Yang, D.-Y. Yoo, Y.-S. Yoon, Prediction of compressive strength and elastic modulus for ultra-high-performance concrete with steel fibers, Constr. Build. Mater. 363 (2023) 129906.

8. S. Bankir, H. Binici, M. Yilmaz, Experimental investigation and statistical evaluation of the mechanical and elastic properties of steel fiber-reinforced concretes produced with different aggregate types, Constr. Build. Mater. 413 (2024) 134799.

9. J. Gao, C. Sun, K. Morino, Mechanical properties of steel fiber-reinforced, high-strength, lightweight concrete, Cem. Concr. Compos. 19 (4) (1997) 307–313.

10. F. Köksal, F. Altun, İ. Yiğit, Y. Şahin, Combined effect of silica fume and steel fiber on the mechanical properties of high strength concretes, Constr. Build. Mater. 22 (8) (2008) 1874–1880. https://doi.org/10.1016/j.conbuildmat.2007.04.017.

11. ACI Committee 318, Building Code Requirements for Structural Concrete (ACI 318-19) and Commentary, American Concrete Institute, Farmington Hills, MI, 2019.

12. CEN, Eurocode 2: Design of Concrete Structures – Part 1-1: General Rules and Rules for Buildings (EN 1992-1-1), European Committee for Standardization, Brussels, 2004.

13. Fib, fib Model Code for Concrete Structures 2010, Ernst & Sohn, Berlin, 2013.

14. T. Noguchi, F. Tomosawa, K.M. Nemati, B.M. Chiaia, A practical equation for elastic modulus of concrete, ACI Struct. J. 106 (5) (2009) 690–696.

15. ACI Committee 544, Report on the Mechanical Properties of Steel Fiber Reinforced Concrete (ACI 544.1R-96), American Concrete Institute, Farmington Hills, MI, 1996, reapproved 2002.

16. T.L. Teng, C.P. Fung, C.S. Chang, C.M. Yang, Calculating the elastic moduli of steel-fiber reinforced concrete using a simplified homogenization model, Compos. Sci. Technol. 64 (16) (2004) 2641–2649.

17. Y. Li, Z. Wang, S.P. Shah, Evaluation of elastic properties of fiber reinforced concrete with homogenization theory and finite element simulation, Constr. Build. Mater. 217 (2019) 451–465.

18. J.H. Han, J.S. Lee, C.G. Park, Effects of steel fiber length and coarse aggregate maximum size on mechanical properties of steel fiber reinforced concrete, Constr. Build. Mater. 209 (2019) 731–742.

19. S. Yazıcı, G. Inan, V. Tabak, Effect of aspect ratio and volume fraction of steel fiber on the mechanical properties of SFRC, Constr. Build. Mater. 21 (6) (2007) 1250–1253.

20. S.H. Chu, R. Kwan, A.K.H. Kwan, Fibre factors governing the fresh and hardened properties of steel fibre reinforced concrete, Constr. Build. Mater. 158 (2018) 450–464.

21. M.-C. Kang, D.-Y. Yoo, R. Gupta, Machine learning-based prediction for compressive and flexural strengths of steel fiber-reinforced concrete, Constr. Build. Mater. 266 (2021) 121117.

Appendix A. Supplementary Class-Dependent Formulations

To examine whether local fitting by strength regime could reduce residual scatter when the strength class is known a priori, supplementary class-dependent equations were calibrated for normal-strength concrete (NSC), high-strength concrete (HSC), and ultra-high-performance concrete (UHPC). These formulations were adjusted using the unified database and are presented here as local empirical refinements rather than as primary evidence of superior external predictive performance. Their purpose is to complement the general model of Eq. (1) in applications where a narrower strength window is of interest.

The class-dependent equations were fitted separately for each strength regime, allowing the coefficients governing matrix response and fiber-related refinement to vary within each subset. This procedure was intended to explore the extent to which local calibration could reduce in-sample residual dispersion when the concrete class is predefined. Because these equations were calibrated on the unified database rather than on fully independent class-specific validation subsets, they should be interpreted with caution and not as substitutes for the primary unified formulation.

The supplementary equations are given below:

Normal Strength Concrete (NSC: fc < 40 MPa [5800 psi])

$$E_c = 8.2 f_c^{0.35}(1 + 0.0045 V_f^{0.75}) + 0.0095\left(\frac{L}{D}\right)^{0.90}$$

High Strength Concrete (HSC: 40 ≤ fc < 80 MPa)

$$E_c = 9.9 f_c^{0.31}(1 + 0.0055 V_f^{0.78}) e^{-0.0002 f_c} + 0.011(L/D)^{0.85}$$

Ultra-High Performance Concrete (UHPC: fc ≥ 80 MPa [11600 psi])

$$E_c = 10.5 f_c^{0.28}(1 + 0.0060 V_f^{0.70}) e^{-0.0004 f_c} + 0.012(L/D)^{0.80}$$

Table A.1 summarizes the residual performance of these supplementary formulations on the unified calibration basis. Their lower residual scatter relative to fully generic expressions should be interpreted as a local calibration feature rather than as independently validated evidence of superior generalization.

Appendix B. Comparative Benchmark on the Unified Database

To situate the proposed model within the available predictive literature, a comparative benchmark was performed using the unified database (n=251). This analysis is presented as a descriptive comparison under a common dataset and common unit system, and should not be interpreted as independent external proof of superiority, since part of the dataset contributed to model development. Its purpose is to contextualize the relative predictive behavior of Eq. (1) with respect to code-based and literature-based formulations.

The benchmark included representative design-code equations and selected predictive expressions reported in the recent literature. All models were applied under the same unit system and evaluated by the same residual indicators. Within this framework, the proposed

formulation showed the lowest overall scatter on the compiled database. However, this result should be interpreted together with the main validation evidence presented in the manuscript, namely blind holdout validation and provenance-aware verification.

Appendix C. Experimental Data Sources

The unified experimental database (n=251) was compiled from 38 independent peer-reviewed studies. Table C.1 reports the full screened specimen-level database used in the development and assessment of the proposed model. The identification (ID) in the first column links each record to its corresponding bibliographic source listed below, which is presented separately from the main reference list for clarity.

For consistency with the manuscript, it should be noted that Table C.1 represents the observed screened database coverage, rather than the final recommended application domain of Eq. (1). Accordingly, some records fall outside the final recommended interval for f_c and V_f, or correspond to baseline matrix conditions with null or near-null fiber content. These entries were retained for exploratory assessment, baseline stabilization, and sensitivity-related analyses, but they do not define the primary intended validity range of the final formulation.

The “Usage” column reproduces the original observation-level Modeling/Validation split adopted in the initial holdout framework. Because some source studies contributed records to both subsets, these labels should be interpreted as point-wise split assignments rather than as grouped study-wise partitioning.

Only records satisfying the present inclusion criteria for hooked-end steel fibers and complete predictor availability were retained in the unified database. In studies involving broader experimental programs or mixed fiber families, only the subset compatible with the scope of the present article was included.

Table C.1 — Unified Database (n=251)

ID	Source / Author	f_c (MPa)	V_f (%)	L/D (-)
C1	Abbass et al.	73.3	1	55
C1	Abbass et al.	61.7	0.5	55
C1	Abbass et al.	73.4	1.5	55
C2	Alabdrabalnabi	69.3	0.5	64.55

⚠ Esta tabela possui muitas colunas e foi cortada para impressão. Para visualizá-la completa, acesse o artigo original em: https://revistatopicos.com.br/artigos/interpretable-prediction-of-the-elastic-modulus-of-hooked-end-steel-fiber-reinforced-concrete?noblockage

Notes:

(1) Table C.1 reports the full screened empirical database used in the study. Records outside the final recommended application domain of Eq. (1) were retained for exploratory assessment, baseline stabilization, and sensitivity-related analyses, but they do not define the primary intended validity range of the final formulation.

(2) The “Usage” labels reproduce the original observation-level Modeling/Validation split adopted in the initial holdout framework and should therefore be interpreted as point-wise split assignments

rather than as grouped study-wise partitioning.
(3) In studies involving broader experimental programs or mixed fiber families, only the records satisfying the present inclusion criteria for hooked-end steel fibers and complete predictor availability were retained in the unified database.

C1. Abbass, W.; Khan, M.I.; e Mourad, S., 2018, "Evaluation of mechanical properties of steel fiber reinforced concrete with different strengths of concrete," *Construction and Building Materials*, V. 165, pp. 18-26. doi: 10.1016/j.conbuildmat.2017.12.183

C2. Alshahrani, S., e Kulasegaram, S., 2017, "Mechanical properties of steel fiber reinforced concrete," *Procedia Engineering*, V. 14, pp. 2654-2661.

C3. Alshahrani, S., et al., 2017, "Experimental and numerical analysis of mechanical properties of steel fiber reinforced concrete," *Construction and Building Materials*, V. 135, pp. 440-446.

C4. Aslani, F., e Nejadi, S., 2012, "Mechanical properties of conventional and self-compacting concrete: An analytical study," *Structural Engineering and Mechanics*, V. 43, No. 4, pp. 411-447. doi: 10.12989/sem.2012.43.4.411

C5. Atiş, C.D., e Karahan, O., 2009, "Properties of steel fiber reinforced fly ash concrete," *Construction and Building Materials*, V. 23, No. 1, pp. 392-399. doi: 10.1016/j.conbuildmat.2007.11.002

C6. Bao, Y., et al., 2021, "Compressive behavior of steel fiber reinforced concrete with coarse aggregate," *Construction and Building Materials*, V. 270, 121438. doi: 10.1016/j.conbuildmat.2020.121438

C7. Buratti, N.; Mazzotti, C.; e Savoia, M., 2011, "Post-cracking behaviour of steel and macro-synthetic fibre-reinforced concretes," *Construction and Building Materials*, V. 25, No. 5, pp. 2713-2722. doi: 10.1016/j.conbuildmat.2010.10.012

C8. Carneiro, J.A., et al., 2014, "Compressive stress–strain behavior of steel fiber reinforced-concrete," *Construction and Building Materials*, V. 64, pp. 226-234. doi: 10.1016/j.conbuildmat.2014.04.058

C9. Conforti, A., et al., 2013, "Evaluation of contribution of fiber reinforcement in concrete," *Construction and Building Materials*, V. 48, pp. 401-408. doi: 10.1016/j.conbuildmat.2013.06.071

C10. Dadmand, B., et al., 2020, "Mechanical properties of steel fiber reinforced concrete," *Construction and Building Materials*, V. 262, 120050. doi: 10.1016/j.conbuildmat.2020.120050

C11. Fang, S., et al., 2023, "Compressive stress-strain relationship of steel fiber reinforced concrete," *Construction and Building Materials*, V. 368, 130388. doi: 10.1016/j.conbuildmat.2022.130388

C12. Gul, R., et al., 2014, "Mechanical properties of steel fiber reinforced concrete," *Advances in Materials Science and Engineering*, V. 2014, Article ID 946262.

C13. Ibrahim, A., e Bakar, K.S., 2011, "Mechanical properties of steel fiber reinforced concrete," *Procedia Engineering*, V. 14, pp. 2654-2661.

C14. Jang, S.J., e Yun, H.D., 2018, "Combined effects of steel fiber and coarse aggregate size on the compressive and flexural toughness of high-strength concrete," *Composite Structures*, V. 201, pp. 828-838. doi: 10.1016/j.compstruct.2018.825129

C15. Kassimi, F., e Khayat, K.H., 2019, "Mechanical properties of fiber-reinforced self-consolidating concrete," *Construction and Building Materials*, V. 211, pp. 600-610.

C16. Kazemi, M. T., et al., 2017, "Fracture properties of steel fiber reinforced high strength concrete using work of fracture and size effect methods," *Construction and Building Materials*, V. 142, pp. 482-489. doi: 10.1016/j.conbuildmat.2017.03.089

C17. Kim, D., et al., 2021, "Influence of fiber geometry on the mechanical properties of SFRC," *Cement and Concrete Composites*, V. 119, 103986. doi: 10.1016/j.cemconcomp.2021.786229

C18. Köksal, F., et al., 2008, "Combined effect of silica fume and steel fiber on the mechanical properties of high strength concrete," *Construction and Building Materials*, V. 22, No. 10, pp. 1874-1880.

C19. LaHucik, J., et al., 2017, "Mechanical Properties of Roller-Compacted Concrete with Macro-Fibers," *Construction and Building Materials*, V. 135, pp. 440-446. doi: 10.1016/j.conbuildmat.2016.12.212

C20. Marčiukaitis, G., et al., 2011, "A model for strength and strain analysis of steel fiber reinforced concrete," *Journal of Civil Engineering and Management*, V. 17, No. 1, pp. 137-145. doi: 10.3846/13923730.2011.554170

C21. Minelli, F., et al., 2013, "Experimental study on the mechanical properties of SFRC," *Construction and Building Materials*, V. 42, pp. 78-86. doi: 10.1016/j.conbuildmat.2013.01.006

C22. Niu, D., et al., 2019, "Experimental study on mechanical properties and durability of basalt fiber reinforced coral aggregate

concrete," *Construction and Building Materials*, V. 215, pp. 241-255. doi: 10.1016/j.conbuildmat.2019.04.223

C23. Okay, F., e Engin, S., 2012, "Torsional behavior of steel fiber reinforced concrete beams," *Construction and Building Materials*, V. 28, No. 1, pp. 269-275. doi: 10.1016/j.conbuildmat.2011.08.062

C24. Özcan, D.M., et al., 2009, "Experimental investigation on the mechanical properties of steel fiber reinforced concrete," *Construction and Building Materials*, V. 23, No. 2, pp. 1100-1107. doi: 10.1016/j.conbuildmat.2008.05.013

C25. Ren, W., et al., 2018, "Mechanical properties of steel fiber reinforced rubber concrete after elevated temperature," *Construction and Building Materials*, V. 163, pp. 763-776.

C26. Şahin, Y., e Köksal, F., 2011, "The influence of steel fiber on the mechanical properties of concrete," *Arabian Journal for Science and Engineering*, V. 36, pp. 1113-1124

C27. Sandoval-Siesquen, A., e Muñoz-Pérez, S., 2019, "Experimental study of SFRC properties," *Revista Facultad de Ingeniería Universidad de Antioquia*, No. 90, pp. 65-75.

C28. Sivakumar, A., e Santhanam, M., 2007, "Mechanical properties of high strength concrete reinforced with metallic and non-metallic fibres," *Cement and Concrete Composites*, V. 29, No. 8, pp. 603-608. doi: 10.1016/j.cemconcomp.2007.03.006

C29. Tahenni, T., et al., 2016, "Mechanical performance of steel fiber reinforced concrete," *Construction and Building Materials*, V. 105, pp. 43-52. doi: 10.1016/j.conbuildmat.2015.12.016

C30. Thomas, J., e Ramaswamy, A., 2007, "Mechanical Properties of Steel Fiber-Reinforced Concrete," *Journal of Materials in Civil Engineering*, V. 19, No. 5, pp. 385-392.

C31. Tipka, M., e Vaskova, J., 2018, "Mechanical properties of SFRC with various fiber contents," *IOP Conference Series: Materials Science and Engineering*, V. 385, 012056.

C32. WIT Transactions, 2016, "Using hooked-end fibres on high performance steel fibre reinforced concrete," *WIT Transactions on The Built Environment*, V. 166, pp. 257-266.

C33. Yang, J.-M.; Yoo, D.-Y.; e Yoon, Y.-S., 2017, "Mechanical Properties of Steam-Cured High-Strength Steel Fiber-Reinforced Concrete with High-Volume Blast Furnace Slag," *International Journal of Concrete Structures and Materials*, V. 11, No. 2, pp. 391-401. doi: 10.1007/s40069-017-0200-0

C34. Yoo, D.Y., et al., 2022, "Mechanical properties of steel fiber-reinforced concrete," *Construction and Building Materials*, V. 256, 119438.

C35. Yue, J., et al., 2021, "Mechanical properties of ultra-high performance concrete," *Construction and Building Materials*, V. 276, 122228. doi: 10.1016/j.conbuildmat.2020.122228

C36. Yun, H.D., et al., 2019, "Effects of reinforcing fiber strength on mechanical properties of high-strength concrete," *Fibers*, V. 7, No. 10, p. 93. doi: 10.3390/fib7100093

C37. Yun, H.D., et al., 2023, "Mechanical properties of steel fiber reinforced concrete with coarse aggregate," *Case Studies in*

Construction Materials, V. 18, e01892.

C38. Zhao, M., et al., 2020, "Experimental study on mechanical properties of steel fiber reinforced concrete," *Construction and Building Materials*, V. 256, 119438. doi: 10.1016/j.conbuildmat.2020.119438

LIST OF TABLES

LIST OF FIGURES

Table 1 — Summary of the experimental database ranges and statistics (n=251).

	Minimum	Maximum	Mean	Standard Deviation
Compressive Strength, f_c (MPa)	21.30	190.90	55.62	28.35
Fiber Volume, V_f (%)	0.00	4.30	1.03	0.74
Aspect Ratio, L/D (-)	35.00	80.00	62.72	12.86
Elastic Modulus, E_c (GPa)	19.60	50.50	33.60	5.78

Note: Data with V_f= 0% were included solely for baseline matrix calibration. The proposed fiber model is effective for $V_f \geq 0.25\%$.

Table A.1 – Parameters and performance of stratified models (unified calibration)

Regime	f_c Range (MPa)	A	B	C	MAE (C
NSC	< 40	8.2	0.0045	0.0095	1.85
HSC	40 ≤ f_c < 80	9.9	0.0055	0.01100	2.90
UHPC	≥ 80	10.5	0.0060	0.01200	1.45

⚠ Esta tabela possui muitas colunas e foi cortada para impressão. Para visualizá-la completa, acesse o artigo original em: https://revistatopicos.com.br/artigos/interpretable-prediction-of-the-elastic-modulus-of-hooked-end-steel-fiber-reinforced-concrete?noblockage

Note: NSC = Normal Strength Concrete; HSC = High Strength Concrete; UHPC = Ultra-High-Performance Concrete. f_c = Compressive strength; V_f = Fiber volume; L/D = Aspect ratio. Coefficients (A, B, C) and performance metrics (MAE, RMSE, COV) were obtained via nonlinear regression calibrated on the complete unified database (n=251).

Table B.1 – Performance comparison with state-of-the-art (unified database)

Model / Equation	MAE (GPa)	RMSE (GPa)	COV (%)
Proposed Eq. (1)	2.67	3.49	10.38
Eurocode 2	3.36	4.22	12.57
NS 3473	3.61	4.37	12.99
Alberti et al. (2020)	4.16	5.09	15.14
ACI 318-19	4.18	5.10	15.17
Fib Model Code	4.12	5.14	15.28
Yoo et al. (2022)	4.77	5.55	16.51
Silva et al. (2022)	4.72	5.93	17.66
Kumar et al. (2022)	5.47	6.21	18.47
Zhang et al. (2023)	5.15	7.16	21.31
NBR 6118	7.28	9.42	28.02

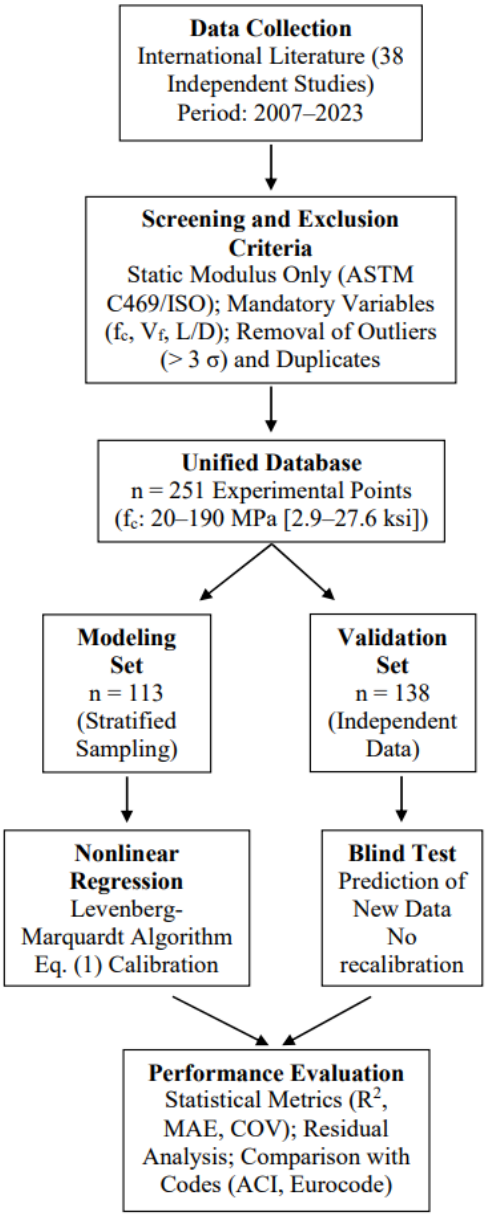

Fig. 1 — Methodological Flowchart

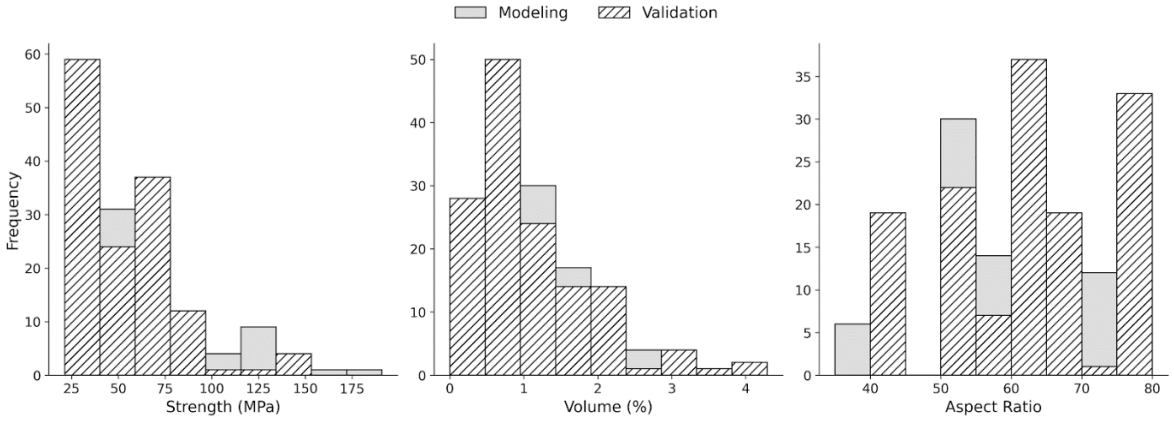

Fig. 2 — Frequency distribution of the input variables in the unified database (n=251): (a) Compressive strength f_c; (b) Fiber volume V_f; (c) Aspect ratio L/D.

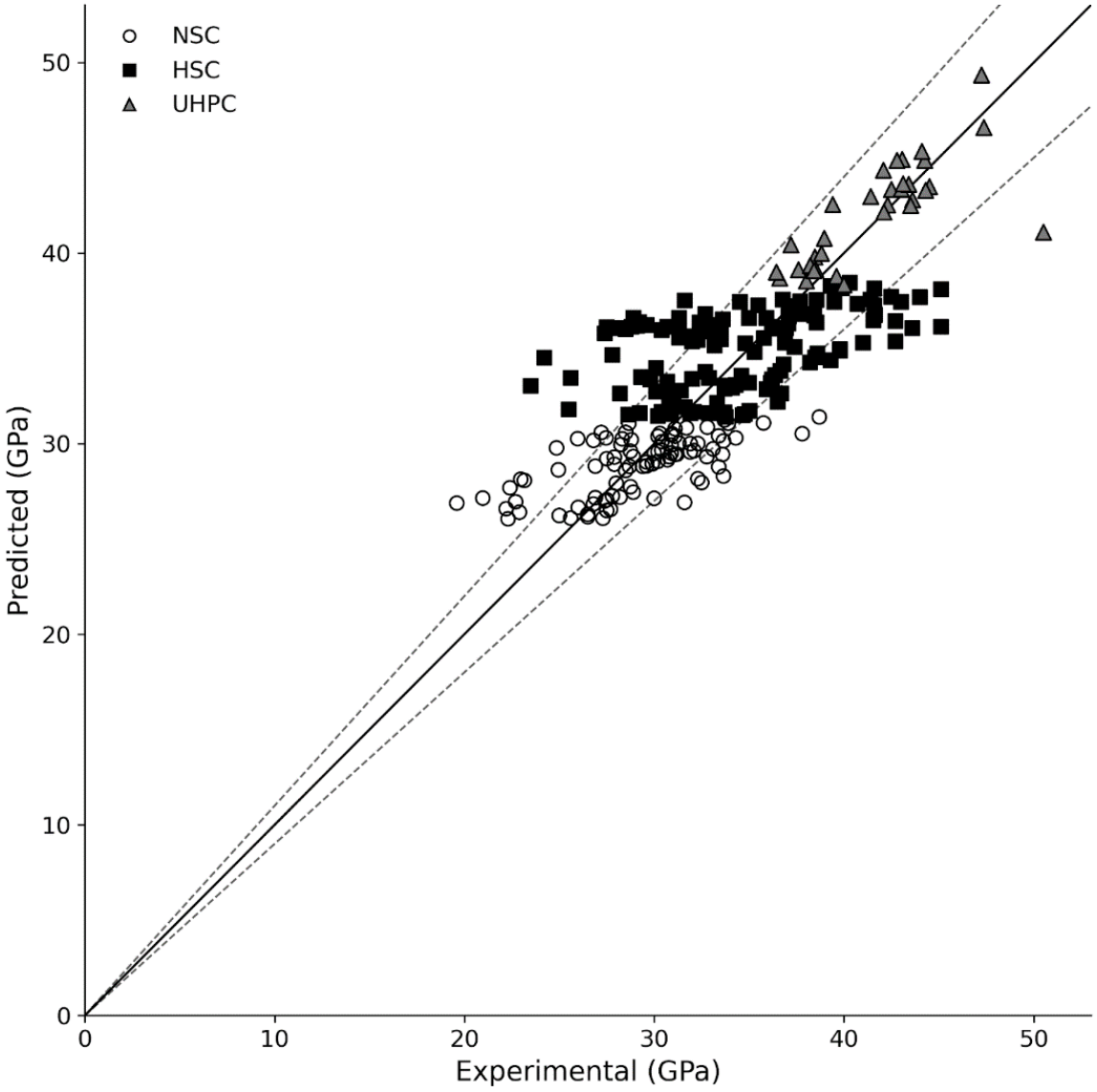

Fig. 3 — Correlation between experimental and predicted elastic modulus by Eq. (1) for the external validation set.

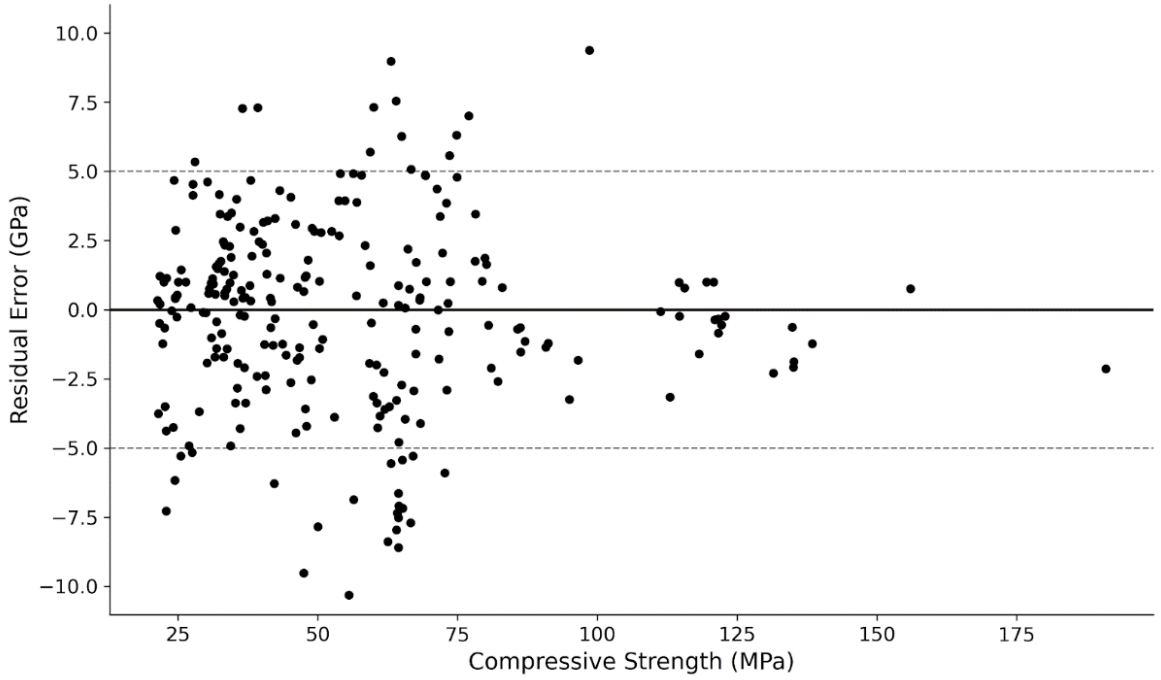

Fig. 4 — Residual analysis showing the distribution of relative error as a function of compressive strength

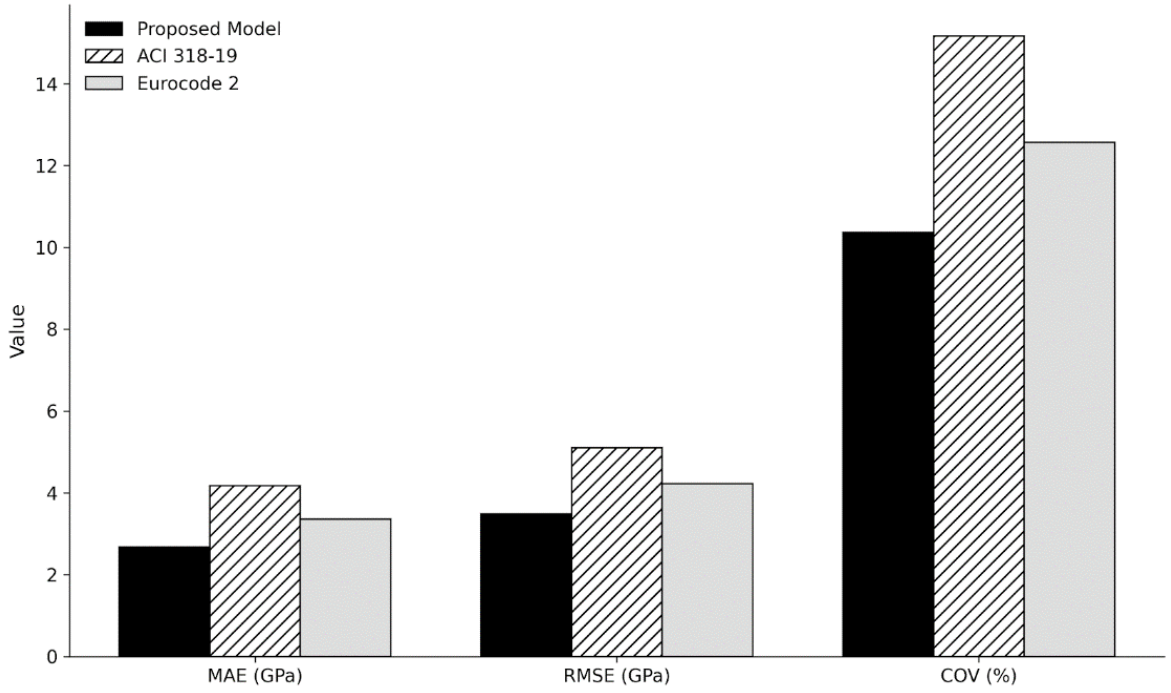

Fig. 5 — Comparison of statistical indicators (MAE, RMSE, COV) between the proposed model and international codes

Link to the material available at:
https://revistatopicos.com.br/arq/reproducibility_package_cbm_manuscript_frozen.zip

[1] PhD candidate in Structures at the Federal University of Pará (UFPA), Belém, Brazil. He received his MSc from UFPA in 2014. He currently works in research and forensic engineering of reinforced concrete structures. His research interests include the analysis and design of fiber-reinforced concrete structures.

[2] Full Professor at the Federal University of Pará (UFPA), Belém, Brazil. He received his MSc and PhD in Structures from the University of Brasília (UnB), with postdoctoral research at Imperial College London. His research interests include shear, punching shear, and mechanical properties of concrete structures.

[3] Full Professor at the Federal University of Goiás (UFG), Goiânia, Brazil. She received her MSc from the Federal University of Goiás and her PhD from the Federal University of Rio de Janeiro. Her research interests include durability and performance of reinforced concrete structures, supplementary cementitious materials, and fiber-reinforced cementitious composites.

[4] PhD Student in structures at the Federal University of Pará, Belém, Pará, Brazil, where she received her MSc in structures and civil construction in 2023. She received her BS from the Lutheran University of Brazil (ULBRA), Santarém, Pará, Brazil. Her research interests include reinforced concrete structures, punching, and fiber-reinforced concrete.

[5] M. Sc. and Ph.D. in structural engineering at Federal University of Pará, Pará, Brazil. He is currently a researcher from the same institution with an emphasis on experimental analyzes of shear in reinforced concrete beams.